

Post-Test Predictions of High Level Vibration Tests of Nuclear Piping

K. R. JAQUAY

Rockwell International Corp., Canoga Park, CA USA

D. F. QUIÑONES

Robert L. Cloud & Associates, Inc., Berkeley, CA USA

H. T. TANG

Electric Power Research Institute, Palo Alto, CA USA

ABSTRACT

Simplified and detailed nonlinear piping analysis methods were used to predict the test behavior of a large-scale modified primary loop of a reactor system at different levels of seismic loading. Test descriptions, analysis techniques, computer models, analysis-to-test comparisons, conclusions and recommendations are presented.

1 INTRODUCTION

A cooperative agreement between the United States (Nuclear Regulatory Commission/Brookhaven National Laboratory (BNL)) and Japan (Ministry of International Trade and Industry/Nuclear Power Engineering Test Center (NUPEC)) led to a 1988 high level vibration test (HLVT) program at NUPEC's Tadotsu Engineering Laboratory on a large-scale modified primary loop of a Pressurized Water Reactor (PWR) system. Testing was run at increasingly higher levels of simulated seismic loading and was stopped before a pressure boundary failure (Kawakami et al. 1989, Park et al. 1991).

Three test segments, two at inelastic load levels, were selected as benchmarks to evaluate nonlinear analysis methods. As part of the U.S. effort, the Electric Power Research Institute (EPRI) cofunded the testing and conducted a post-test prediction evaluation project using both simplified and detailed nonlinear solutions.

The simplified nonlinear solutions used the "refined" incremental hinge method (IHM) developed by EPRI (Jaquay and Tang 1988, Jaquay and Castle 1990). The detailed nonlinear solutions used the ABAQUS computer code (Hibbitt et al. 1991).

2 TEST DESCRIPTION

The HLVT test article is a modification of a 1/2.5-scale model PWR Primary Coolant Loop used in Japanese proving tests (Fujita et al. 1989). The steam generator (SG) was cut off just above the middle shell support, the support removed and the lower column support structure replaced by a pivot assembly. These modifications would permit the truncated SG to rotate freely in the direction allowed by the pivot were it not for the attached piping. Reinforcement was added to the steam generator support system halfway through the HLVT test matrix due to observed support slippage. Fig. 1 shows the setup.

The piping was 334 mm to 377 mm (≈ 14 inch) outside diameter with 27.5 mm to 31.1 mm (roughly Schedule 80) wall thickness. It is 300 Series cast stain-

SMIRT 11 Transactions Vol. K (August 1991) Tokyo, Japan, © 1991

less steel. The SG is ferritic steel and the reactor coolant pump (RCP) is stainless and ferritic steel. The piping was pressurized to 157 kg/cm².

18 HLVT test runs were conducted using the Tadotsu Large-Scale Vibration Table Facility as outlined in Table 1. Four different three second shaker table time history segments were developed by BNL and designated as A,B,C and D input waves (Hofmayer et al. 1989), each with a different frequency content. The maximum test level was identified as 1.0MPR (Maximum Plastic Run).

After Test Run 11, fatigue cracks were observed at the top outside surface of the hot leg piping in a tapered region where the thicker elbow was welded to the straight pipe spool (Kawakami et al. 1989). About a dozen circumferential cracks up to 15 mm in length and 2.5 mm in depth were observed. The cracks proceeded to grow in subsequent test runs to form a single major crack. The tests were terminated after the first segment of Test Run 14 when this crack had grown 94% through the wall. Fig. 2 is a longitudinal section circumferentially adjacent to the location of maximum crack depth. Fig. 3 is a cross section through the SG end of the hot leg piping.

The test segments selected for the benchmark evaluations were the Segment A portions of Runs 4, 8** and 11, designated as the 0.1MPR, 0.4MPR and 1.0MPR benchmark runs respectively. BNL provided EPRI shaker table accelerometer records and Fig. 4 is response spectra curves developed from these records.

3 ANALYSIS TECHNIQUES

3.1 Incremental hinge method

The incremental hinge method (IHM) uses limit analysis concepts to define a response load versus ductility curve and inelastic response spectra concepts to define an input load versus ductility curve. The intersection of the two curves defines the effective plastic load level.

To develop the response load curve, a series of conventional response spectrum solutions are performed with moment hinges incrementally added to the model. The seismic loading is first applied to the model as a conventional linear elastic response spectrum (LERS). The LERS loading is scaled downward until a location has just reached its dynamic hinge moment per data from tests of piping components (General Electric 1989). A moment hinge is placed at this first hinge location and an increasing magnitude flat response spectrum (FRS) is applied to this new 1-hinge model. When the combined level of load from the scaled LERS loading and the increasing FRS loading reaches that which causes a second location to reach its hinge moment, a second hinge is placed in the model and the solution continues with increasing FRS loading, adding hinges as they occur. Displacement ductility is plotted against the response acceleration to create the response load curve.

The input load curve for the IHM is developed using the reduction factors developed by Riddell and Newmark (1979) for nonlinear systems. The "refined" IHM also uses a ductility-based frequency shift (Lazzeri 1987).

The input load curve starts at the acceleration on the response spectrum curve at the dominant modal frequency. For varying ductility, the frequency shift is computed and the elastic acceleration response at the shifted frequency is reduced by the Riddell-Newmark factor. Fig. 5 is the response load curve and 3% elastically damped input load curves for the HLVT.

3.2 Time history analyses

The 0.1MPR test did not exhibit any significant nonlinear behavior and was evaluated using the linear *MODAL DYNAMICS option of the ABAQUS program. The 0.4 MPR and 1.0 MPR tests were evaluated using the nonlinear implicit inte-

gration procedure in the *DYNAMICS option of the ABAQUS program.

The *MODAL DYNAMICS option in ABAQUS integrates the modal amplitudes through time and the response is synthesized from these modal responses. The technique used in ABAQUS to extract eigenmodes is the subspace iteration method. Since over 99.5% of the HLVT response was contributed by the second mode, the eigenvalue extraction only requested the first two modes. A time step of 0.005 seconds was used.

The nonlinear implicit integration procedure for the *DYNAMICS option in ABAQUS uses the Hilber-Hughes-Taylor implicit operator which is a single parameter operator with controllable numerical damping. A value of $-1/3$ was selected for the numerical damping and analysis was carried out using fixed time steps of 0.005 seconds. The total CPU time for each solution was around 18 hours and several restarts were used to work through the solution.

Two plasticity models were used for the 1.0MPR solution and one for the 0.4MPR solution. Both solutions were conducted using a Mises yield surface, isotropic hardening and a bilinearized stress-strain curve developed from tension tests on the same heats of material used in the HLVT hot leg. The 1.0MPR solution was also run using kinematic hardening with a tenth-cycle isotropically hardened yield chosen for each element based on an a-priori estimate of the average element strain range.

4 COMPUTER MODELS

Fig. 6 is a computer plot of the SAP86 (Number 1986) model used in the IHM solution. Except for the hot leg, the ABAQUS model is very similar. A mesh convergence check of the models was conducted using refined models that doubled the number of elements. The maximum difference in the first five modal frequencies between the coarse and fine models was less than 0.1%. Predictions of the second mode frequencies were within 7% of the test values for the SAP86 model and within 3% of the test values for the ABAQUS model. Fig. 7 is the ABAQUS second mode plot.

Fig. 8 is the SAP86 hot leg model. The elbow was modeled with a varying thickness to correct the flexibility for end effects and reduced curvature.

The ABAQUS hot leg model is shown in Fig. 9. ELBOW31 elements were used with 7,18 and 6 integration points through the thickness, around the circumference and along the length of each element, respectively. Axial mesh refinement was used at the predicted high stressed tapered transition section, however, the pipe elements were not suitable for modeling the geometric discontinuity in outer diameter, and much less so the variable thickness of the elbow (the bore of the elbow was eccentric to the outer diameter).

5 PREDICTION VERSUS TEST COMPARISON

Both analysis methods were far better at predicting the dynamic behavior of the dominant X-direction second mode than they were at predicting the dynamic behavior of lower magnitude "cross modes". Displacement and acceleration predictions in the X-direction were in excellent agreement with the measured values. Predictions in the Y-direction were often in error by factors of 3 to 8, however, these errors were at the top of the SG where anomalies in the data suggests that the SG pivot support may have introduced "noise".

Both analysis methods underpredicted the RCP snubber test loads, the IHM averaging about 20% low and ABAQUS averaging about 40% low.

Both analysis methods correctly identified the highest strain ranges as occurring at the failure location in the tapered transition joint (TTJ). The IHM predicted strain ranges were very close to the test data due to the availability of good peak stress indices for the TTJ discontinuity, while the

ABAQUS predictions were understandably low due to the TTJ geometric discontinuity missing from the model.

One disturbing result of the comparisons was the poor ABAQUS agreement with strain data in the hot leg elbow. ABAQUS indicated a significant ratchet mechanism existed while the test data showed none, even though the strain ranges were of similar magnitude (see Figs. 10 and 11). This was true for both the hoop and axial direction, for both hardening models and for both the 0.4 and 1.0MPR solutions.

Probably the most meaningful comparisons are those for the maximum test measured values of displacements, accelerations, forces and strain ranges. Fig. 12 plots these comparisons and includes a set of SAP86 linear response spectrum predictions as a reference. The nonlinear behavior is evident in the linear solutions' overprediction of loads and underprediction of strains. Overall, both nonlinear method predictions provided reasonably good indications of maximum response.

6 CONCLUSIONS AND RECOMMENDATIONS

The EPRI HLVT post-test prediction evaluation has demonstrated that reasonable predictions of the overall magnitude of nonlinear system response can be established using the IHM and ABAQUS analysis methods. Particularly good predictions of displacements and accelerations in the predominant modes can be expected. However, two inconsistencies between the predictions and test were noted that requires further study. First, the ability of the methods to adequately predict lower magnitude "cross modes" needs to be assessed, possibly by linear studies. Second, the root cause for the ABAQUS erroneous prediction of a plastic ratchet mechanism needs to be understood.

REFERENCES

- Fujita, K., et al. (1989). Proving Test on the Seismic Reliability for the PWR Primary Coolant Loop System. PVP-Vol.182, pp. 303-308.
- General Electric Nuclear Co. Report (1989). Piping and Fitting Dynamic Reliability Program, Vol. 2 - Component Test Report. EPRI RP 1543-15.
- Hibbitt, D. et al. (1991). ABAQUS-EPGEN: A General Purpose Finite Element Code. EPRI NP-7252-CCM-L.
- Hofmayer, C., et al. (1989). High Level Vibration Test of Nuclear Power Piping Overall Plan, Input Motion Development and Analysis. SMiRT 10, Vol.5, p.93.
- Jaquay, K.R. and Tang, H.T. (1988). Improved Load Definitions for Incremental-Hinge-Based Nonlinear Piping Analysis Methods. Second Symposium on Current Issues Related to Nuclear Plant Structures, Equipment and Piping. p.10-1.
- Jaquay, K.R. and Castle, W.R. (1990). A Simplified Inelastic Seismic Analysis Method for Piping Systems. EPRI NP-6809.
- Kawakami, S. et al. (1989). High Level Vibration Test of Nuclear Power Piping - Test Procedure and Test Results. SMiRT 10, Vol.K2, p. 745.
- Lazzeri, L. (1987). Design Considerations for the Analysis of Piping in Dynamic Conditions with Moderate Ductility. PVP-Vol.127, p. 207.
- Number Cruncher Microsystems, Inc. (1986). SAP86, A Finite Element Program for Static and Dynamic Analysis of Linear Structural Systems.
- Park, Y.J. et al. (1991). The High Level Vibration Test Program Final Report. NUREG/CR-5585.
- Ridell, R. and Newmark, N.M. (1979). Statistical Analysis of the Response of Nonlinear Systems Subjected to Earthquakes. University of Illinois.

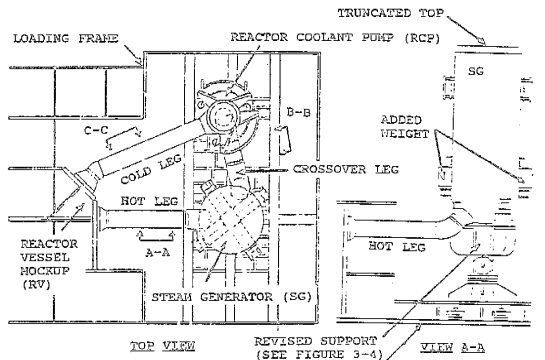


Fig. 1 HLVT test setup

Table 1 HLVT program

Run identifier	Input wave segments	MPR target level	Peak acceleration gals	Peak acceleration g/s
2	A-B-C-D	0.07	150	0.15
3	A-B-C	0.10	195	0.19
4	A-B-C-D	0.10	195	0.19
5	A-B-C-D	0.20	390	0.40
6	A-B-C-D	0.30	705	0.72
7	A-B-C-D	0.35	741	0.76
8	A-B-C-D	0.40	816	0.92
9*	A	0.60	1250	1.28
9**	A	0.80	1850	1.89
10*	A	1.00	2350	2.40
SG supports reinforced				
8*	A-B-C-D	0.40	829	0.85
8**	A-B-C-D	0.40	1099	1.12
9	A-B-C-D	0.75	1786	1.82
10	A-B-C-D	1.00	2420	2.47
11	A-B-C-D	1.00	2431	2.48
12	A-B-C-D	1.00	2431	2.48
13	A-B-C-D	1.00	2431	2.48
14*	A	1.00	2310	2.36

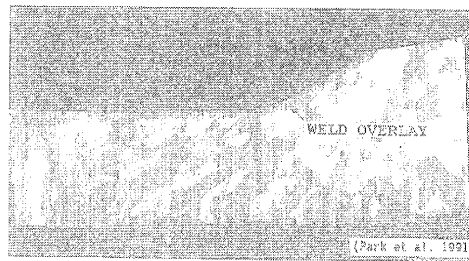
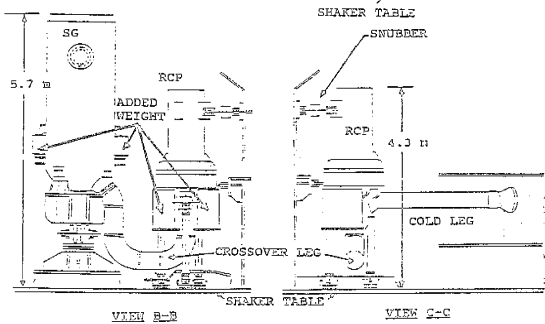


Fig. 2 Crack location

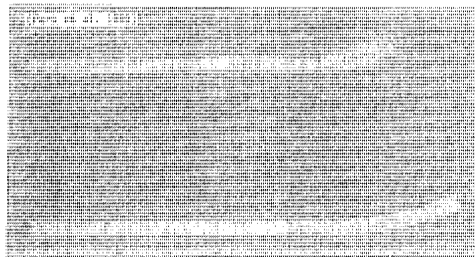


Fig. 3 Hot leg section

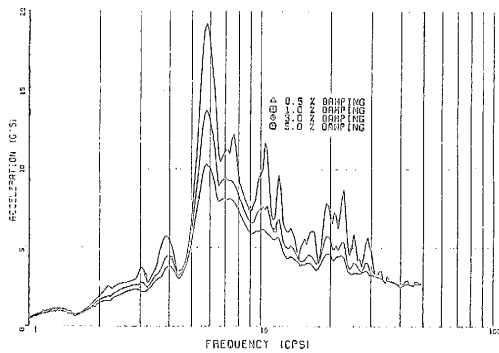


Fig. 4 HLVT 1.0MPR spectra

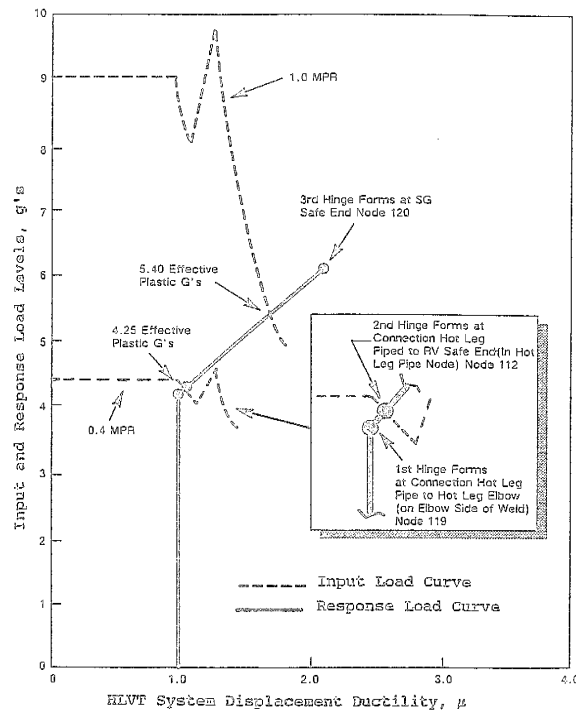


Fig. 5 HLVT INM solution

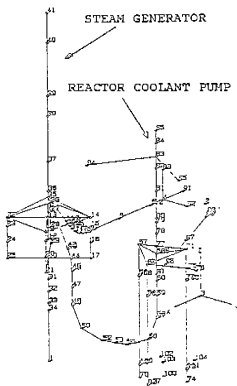


Fig. 6 SAP86 model

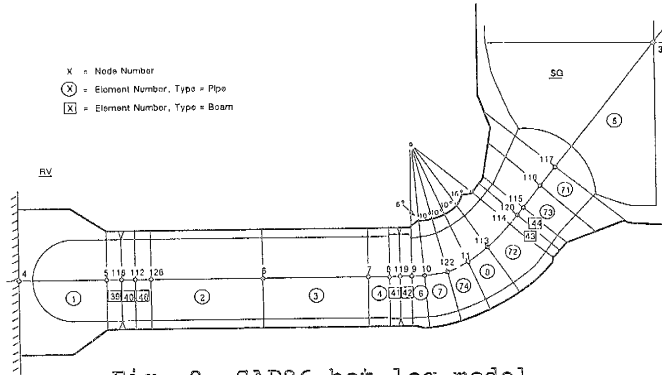


Fig. 8 SAP86 hot leg model

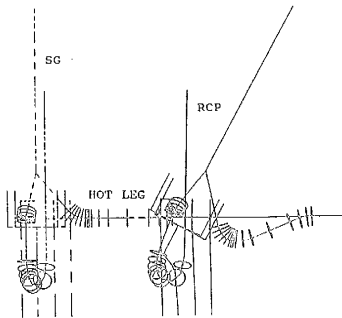


Fig. 7 ABAQUS 2nd mode

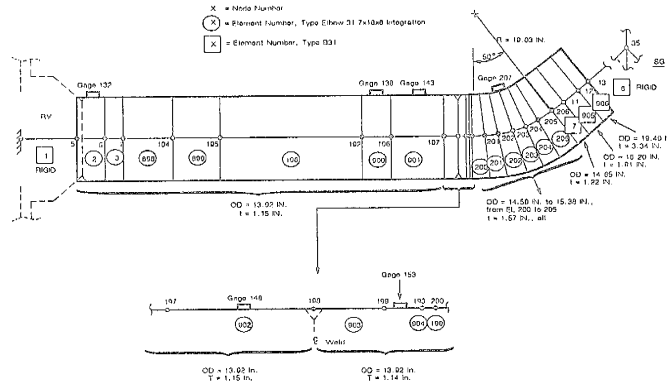


Fig. 9 ABAQUS hot leg model

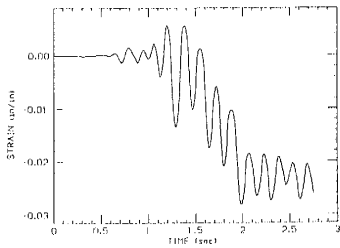


Fig. 10 Predicted HL elbow axial strain

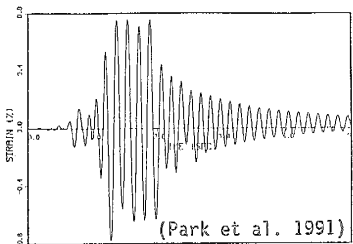


Fig. 11 Measured HL elbow axial strain

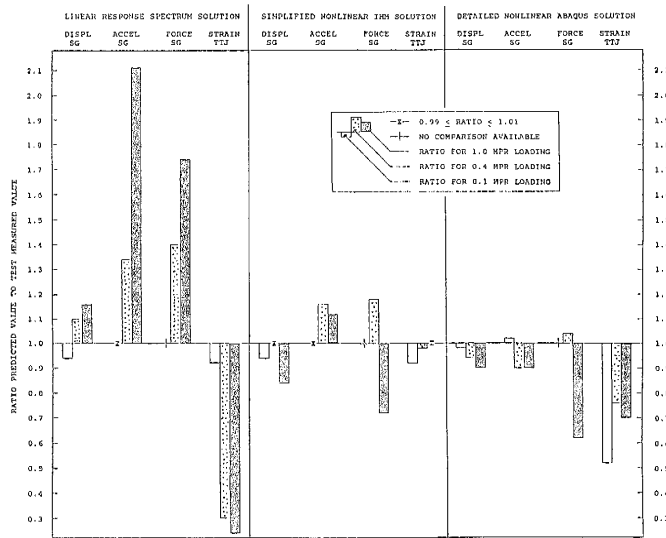


Fig. 12 HLVT maximum value comparison